Indian Journal of Advances in Chemical Science

Article

Synthesis and Characterization of Iron(II) Coordination Complexes with PPh2Py and DPEphos Ligands: A Combined Experimental and Theoretical Study

Malabika Borah[1], Nabanita Saikia[2]*, Pankaj Das[3]

[1]Department of Chemistry, B. N. College, Dhubri, Assam, India, [2]Department of Chemistry, New Mexico Highlands University, Las Vegas, New Mexico, United States, [3]Department of Chemistry, Dibrugarh University, Dibrugarh, Assam, India

ABSTRACT

The synthesis and characterization of Iron(II) complexes [$FeCl_2(\eta^2$-P,N-$PPh_2Py)_2$] (**1**) and [$FeCl_2(\eta^2$-P,P-DPEphos)$_2$] (**2**), with PPh_2Py and DPEphos ligands, were performed using elemental analysis, ESI-mass, Fourier transform infrared spectra (FTIR), ultraviolet-visible, ^1H and $^{31}P\{^1H\}$ nuclear magnetic resonance spectroscopy. FTIR measurements predicted *cis*-isomer to be the most stable form of complex **1** and *trans*-isomer to be the most stable form of complex **2**. Quantum chemical calculations using first-principles density functional theory were performed on the two complexes at the B3LYP/LANL2DZ/6-31+G(d,p) level of theory. Theoretical calculations predicted that the ground state of the complexes would be a quintet spin state. However, in complex **1**, the quintet spin state led to a significant elongation in Fe–P bond length to ~3.55 Å. Thus, a singlet (S = 1/2) spin state was considered for complex **1** which showed reasonable agreement with calculated geometric parameters. *Trans*-configuration of complex **2** was shown to have a higher highest occupied molecular orbital-lowest unoccupied molecular orbital energy gap (higher stability) than complex **1** which was attributed to the nature of the ligand coordinated to Fe(II) ion.

Key words: Fe(II) complexes, PPh2Py and DPEphos ligands, elemental analysis, Fourier Transform Infrared spectra, NMR spectroscopy, Density Functional Theory.

1. INTRODUCTION

Transition metal complexes with hemilabile ligands have garnered significant interest due to their diverse structures, unusual reactivity, and catalytic applications. The bite angle of hemilabile ligands plays an important role in determining their reactivity. For example, the PPh_2Py ligand has been widely used as a bridging ligand because of its rigidity, which is induced by a small bite angle in a chelated mode, thereby, favoring the formation of a metal–metal bond [1-3]. The coordination modes of this ligand have been reported, which include P-monodentate [4,5], P,N-chelate [5,6], P,N-bridging [7-9], and N-monodentate [10]. Several examples of pyridylphosphine coordinated homo- and hetero-binuclear complexes with transition metals have also been investigated [11-13]. On the other hand, the coordination chemistry of large bite-angle diphosphine ligands finds applications as catalysts in many organic transformation reactions [14]. DPEphos ligand, with a large bite angle, has been widely used due to its rich coordination behavior stemming from the presence of two phosphorus atoms and an oxygen atom as potential donor sites. Several coordination modes of this ligand have been reported such as P-monodentate [15], P,P-chelate [15-17], P,O,P-chelate [17,18], and P,P-bridging [17,19]. Literature suggests that this ligand can form coordination compounds with a variety of transition metals such as Cu(I) [15,20-22], Ni(0) [23], Ni(II) [22], Rh(I) [24,25], Ru(II) [17], Ag(I) [19,26], Pd(0) [27], Pd(II) [16], and Re(II) [28-30]. Some of these complexes serve as excellent catalysts for hydrogenation [17,28], hydroformylation [31], carbonylation [24,25], aryl halide amination [32,33], and cross-coupling [34] reactions.

To the best of our knowledge, coordination compounds of iron with phosphine ligands, such as diphenyl-2-pyridylphosphine (PPh_2Py) and (bis-2-diphenylphosphinophenyl)ether (DPEphos), are rather limited [11,35]. This served as a motivation for the present study. We synthesized Fe(II) complexes with PPh_2Py and DPEphos ligands and the complexes were characterized using elemental analysis, ESI-mass, Fourier transform infrared spectra (FTIR), Ultraviolet (UV)-visible, ^1H and $^{31}P\{^1H\}$ nuclear magnetic resonance (NMR) spectroscopy. Further, first-principles density functional theory (DFT) calculations were performed on the *cis*- and *trans*-isomers, and the results were compared with experimentally synthesized complexes. DFT calculations in the gas phase offered a detailed understanding of the most stable geometrical isomers and insights into the structure and electronic properties of the Fe(II) complexes.

2. EXPERIMENTAL

2.1. Materials

The starting materials, diphenyl-2-pyridylphosphine (PPh_2Py), and (bis-2-diphenylphosphinophenyl)ether (DPEphos) were purchased from M/S Aldrich, USA. $FeCl_2.4H_2O$ was purchased from across

***Corresponding author:**
Nabanita Saikia,
E-mail: nsaikia@nmhu.edu

ISSN NO: 2320-0898 (p); 2320-0928 (e)
DOI: 10.22607/IJACS.2024.1203006

Received: 15th June 2024;
Revised: 08th July 2024;
Accepted: 05th August 2024;
Published: 05th September 2024

chemicals. All other chemicals and solvents were purchased from different Indian firms. The solvent was distilled and dried before use.

2.2. Synthesis of Complexes

2.2.1. Synthesis of $[FeCl_2(\eta^2\text{-}P,N\text{-}PPh_2Py)_2]$ (1) complex

A solution of the ligand PPh_2Py (250 mg; 0.95 mmol) in DMF (15 mL) was added to a solution of $FeCl_2.4H_2O$ (100 mg; 0.50 mmol) in 10 mL DMF. The reaction mixture was stirred and refluxed under a continuous flow of N_2 for an hour. The resulting solution was evaporated after cooling and washed several times with ether and DCM to obtain a reddish-colored complex (69% yield).

Analytical values for $C_{34}H_{28}N_2P_2Cl_2Fe$ (%): C, 62.48; H, 4.29; N, 4.29; Found: C, 61.99; H, 4.14; N, 3.97. ESI-mass, m/z (%): $[M\text{-}2Cl\text{-}1]^+$, 581 (100%); $[M\text{-}2Cl\text{-}PPh_2Py\text{-}1]^+$, 318 (3%); $[M\text{-}2Cl\text{-}PPh_2Py\text{-}Fe+1]^+$, 264 (5%); $[M\text{-}2PPh_2\text{-}3]^+$, 280 (5%); $[M\text{-}Cl\text{-}2PPh_2+2]^+$, and 249 (5%). Selected IR frequencies (cm^{-1}, KBr): 540 (υ_{FeP}), 318, 293 (υ_{FeCl}). UV-Vis (CH_3CN), λ_{max}(nm): 300, 536. ^1H NMR (δ ppm): 8.67 (br, 8H, Py), 5.73–6.05 (br, 20H, Ph). $^{31}P\{^1H\}$ NMR (δ ppm): −7.57(s).

2.2.2. Synthesis of $[FeCl_2(\eta^2\text{-}P,P\text{-}DPEphos)_2]$ (2) complex

10 mL DMF solution of $FeCl_2.4H_2O$ (100 mg; 0.50 mmol) was added to 15 mL DMF solution of the ligand DPEphos (550 mg; 1.02 mmol). The resulting mixture was refluxed under N_2 for an hour. After cooling, the solution was evaporated, and the product was washed several times with ether and DCM to obtain a reddish-brown complex (38% yield).

Analytical values for $C_{64}H_{56}O_2P_4Cl_2Fe$ (%): C, 71.70; H, 4.65; Found: C, 71.26; H, 4.37. ESI-mass, m/z (%): $[M\text{-}1]^+$, 1204 (12%); $[M\text{-}2Cl\text{-}Ph+2]^+$, 1059 (32%); $[M\text{-}2Cl\text{-}Ph\text{-}PPh_2]^+$, 872 (5%); $[M\text{-}2Cl\text{-}3Ph\text{-}PPh_2\text{-}O\text{-}1]^+$, 702 (100%); $[M\text{-}2Cl\text{-}3PPh_2\text{-}O\text{-}PPh\text{-}P\text{-}2]^+$, 593 (45%). Selected IR frequencies (cm^{-1}, KBr): 567 (υ_{FeP}), 318 (υ_{FeCl}). UV-Vis (CH_3CN), λ_{max}(nm): 315. ^1H NMR (δ ppm): 5.13–5.29 (br, 56H, Ph). $^{31}P\{^1H\}$ NMR (δ ppm): 30.05(s).

2.3. Physical Measurements

The IR spectra were recorded in the KBr disc and in $CHCl_3$ using Shimadzu IR-prestige-21 (4000–250 cm^{-1}). The UV-Vis spectra of the complexes were recorded using Shimadzu, graphicord UV-240, and Shimadzu UV 1700 spectrophotometers. The electrospray mass spectra of the complexes were recorded using Waters ZQ-4000 LC-Mass spectrometer. The ^1H and ^{31}P NMR spectra of the complexes were recorded using TMS and 85% H_3PO_4 as a reference, respectively, by Bruker Avance 400 MHz spectrometer.

2.4. Theoretical Calculations

Since repeated attempts to obtain diffraction quality crystals of the two Fe(II) complexes failed at the level of the experiment, using an approach outlined in previous studies [11,35], we modeled the *cis*- and *trans*-isomers of the Fe(II) complexes by substituting the two bulky phenyl groups in PPh_2 by hydrogen atoms [Scheme 1]. This made the calculations easier to handle and reduced both the time and cost of calculation. The initial geometries of Fe(II) complexes with hemilabile phosphine-based ligands, PPh_2Py, and DPEphos were optimized in the gas phase without any symmetry constraints using the Gaussian 09 program [36]. Spin states, namely singlet (S = 1/2), triplet (3/2), and quintet (5/2), were considered to determine the ground state of Fe^{2+} complexes. The hybrid generalized gradient approximation exchange-correlation functional, B3LYP (Becke, 3-parameter, Lee–Yang–Parr) was employed without any symmetry constraint along with the non-relativistic effective core potential LANL2DZ (Los Alamos effective-core potential) basis set [37] for Fe and Cl atoms and a 6–31+G (d,p) basis set for C, H, O, and P atoms. The geometry optimization was followed by frequency calculations to confirm the ground state of the optimized structures.

The reliability of B3LYP functional for studying a wide range of molecular properties including electronic structures of biomolecules interacting with metal nanoclusters has been reported [38,39] and showed consistent results for complexes with gold and other transition metals [40,41]. The electronic properties, frontier molecular orbitals, namely highest occupied molecular orbital (HOMO), lowest unoccupied molecular orbital (LUMO), HOMO-1, HOMO-2, LUMO+1, LUMO+2, and HOMO-LUMO energy gap of the complexes were calculated. GaussView 6.0 was employed for all structural analysis. The minimum energy structures of the complexes were visualized using GaussView and the frontier molecular orbitals were visualized using Avogadro software, version 1.2.0 [42].

3. RESULTS AND DISCUSSION

3.1. Synthesis of Complexes

The synthesis route of the complexes is shown in Scheme 1. The reaction of $FeCl_2.4H_2O$ with two molar equivalents of PPh_2Py and DPEphos ligands in DMF solution yields hexa-coordinated $[FeCl_2(\eta^2\text{-}P,N\text{-}PPh_2Py)_2]$ (1) and $[FeCl_2(\eta^2\text{-}P,P\text{-}DPEphos)_2]$ (2) complexes where both ligands were coordinated in a bidentate fashion.

The ESI-mass spectrum of $[FeCl_2(\eta^2\text{-}P,N\text{-}PPh_2Py)_2]$ (**1**) shows a base peak at m/z = 581 (100%) which corresponds to the $[Fe(PPh_2Py)_2+1]^+$ fragment, *that is,* $[M\text{-}2Cl\text{-}1]^+$ ion, formed by the removal of two Cl^- ions from the complex. Low intense peaks are observed at *m/z* = 318, 280, 264, 249, respectively, which are due to $[M\text{-}2Cl\text{-}PPh_2Py\text{-}1]^+$, $[M\text{-}2PPh_2\text{-}3]^+$, $[M\text{-}2Cl\text{-}PPh_2Py\text{-}Fe+1]^+$, and $[M\text{-}2PPh_2\text{-}Cl+2]^+$ ions, respectively [Supporting Information, Figures S1 and 2]. The ESI-mass spectrum of $[FeCl_2(\eta^2\text{-}P,P\text{-}DPEphos)_2]$ (**2**) shows a low intense $[M\text{-}1]^+$ peak at m/z = 1204. The base peak at m/z = 702 is due to the $[M\text{-}2Cl\text{-}3Ph\text{-}PPh_2\text{-}O\text{-}1]^+$ fragment. Peaks with moderate intensities are observed at *m/z* = 1059 and 593 due to the $[M\text{-}2Cl\text{-}Ph+2]^+$ and $[M\text{-}2Cl\text{-}3PPh_2\text{-}O\text{-}PPh\text{-}2]^+$ ions, respectively. In addition, a peak at *m/z* = 872 is observed for $[M\text{-}2Cl\text{-}Ph\text{-}PPh_2]^+$ fragment with a very low intensity [Supporting Information, Figures S3 and 4]. The fragmentation patterns of both complexes are consistent with similar types of mononuclear dichloride complexes.

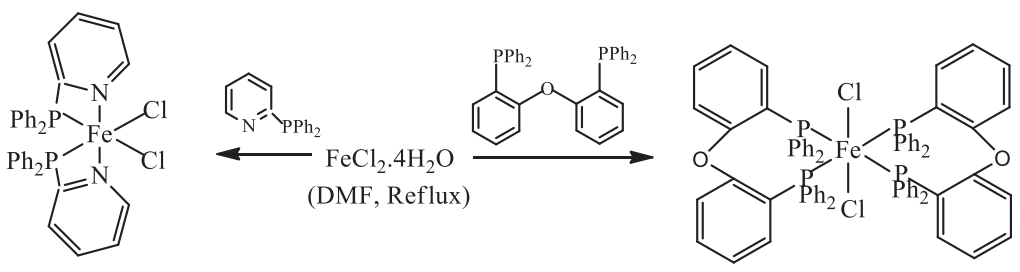

1 **2**

Scheme 1: General scheme for the synthesis of complexes **1** and **2**.

The elemental analysis and ESI-mass spectra of the complexes are in clear agreement with the above formulation.

3.2. FTIR Studies

The IR spectrum of $[FeCl_2(\eta^2\text{-P,N-PPh}_2Py)_2]$ (**1**) in KBr exhibits a characteristic M-P stretching band at 540 cm^{-1} consistent with coordination of the ligand through P–atoms [Figure 1a]. The spectrum shows a pyridine ring deformation frequency $\{\nu_{C=N}\}$ at 1614 cm^{-1} which shifts to higher frequency in comparison to the free PPh_2Py ligand (1567 cm^{-1}) indicating the presence of N-coordinated pyridine rings [6,43]. The far IR shows two M–Cl stretching bands at 318 and 293 cm^{-1}, respectively, which are characteristic of the *cis*-arrangement of chlorides [44].

In the IR spectrum of $[FeCl_2(\eta^2\text{-P,P-DPEphos})_2]$ (**2**), a very low-intensity M–P stretching band is observed at 567 cm^{-1} [Figure 1b]. An intense M–Cl stretching peak in the far IR spectrum at 318 cm^{-1} is consistent with the chlorides in a *trans*-arrangement [44]. The non-coordination of the ethereal oxygen is further confirmed by the presence of the band at 1122 cm^{-1} [45].

3.3. UV-Vis Studies

UV–Vis spectrum of $[FeCl_2(\eta^2\text{-P,N-PPh}_2Py)_2]$ (**1**) in methanol shows two intense bands at 300 and 536 nm [Figure 2a]. The band at 300 nm is attributed to intra-ligand n→π* transition which is slightly shifted to higher wavelength region compared to free ligand while the band at 536 nm is due to LMCT transition. The UV–Vis spectrum of $[FeCl_2(\eta^2\text{-P,P-DPEphos})_2]$ (**2**) in DMSO shows a strong absorption band at 315 nm which can be assigned to intra-ligand n→π* transition [Figure 2b]. This band shifts about 46 nm in comparison to free ligand and is attributed to the coordination with Fe(II).

3.4. ^1H and $^{31}P\{^1H\}$ NMR Studies

The $^{31}P\{^1H\}$ NMR spectrum of $[FeCl_2(\eta^2\text{-P,N-PPh}_2Py)_2]$ (**1**) shows a strong singlet at δ–7.57 ppm indicating the presence of only one type of P-atoms in the complex [Figure 3a]. Compared to the $^{31}P\{^1H\}$ NMR spectrum of free ligand [46], complex **1** shows an upfield shift which is characteristic of a four-membered chelated ring [6]. A similar type of complex was reported by Ndifon *et al*. [43] where they established using IR spectroscopy that each PPh_2Py ligand in the complex is η^1-coordinated through N-atom and not through P-atom. The ^1H NMR spectrum shows a broad peak for the pyridyl protons centered at δ 8.67 ppm, shifting downfield compared to the free ligand which indicates the coordination through N-atom [Supporting Information, Figure S5]. Thus, both $^{31}P\{^1H\}$ and ^1H NMR spectra support our proposed η^2-P,N-structure of the complex.

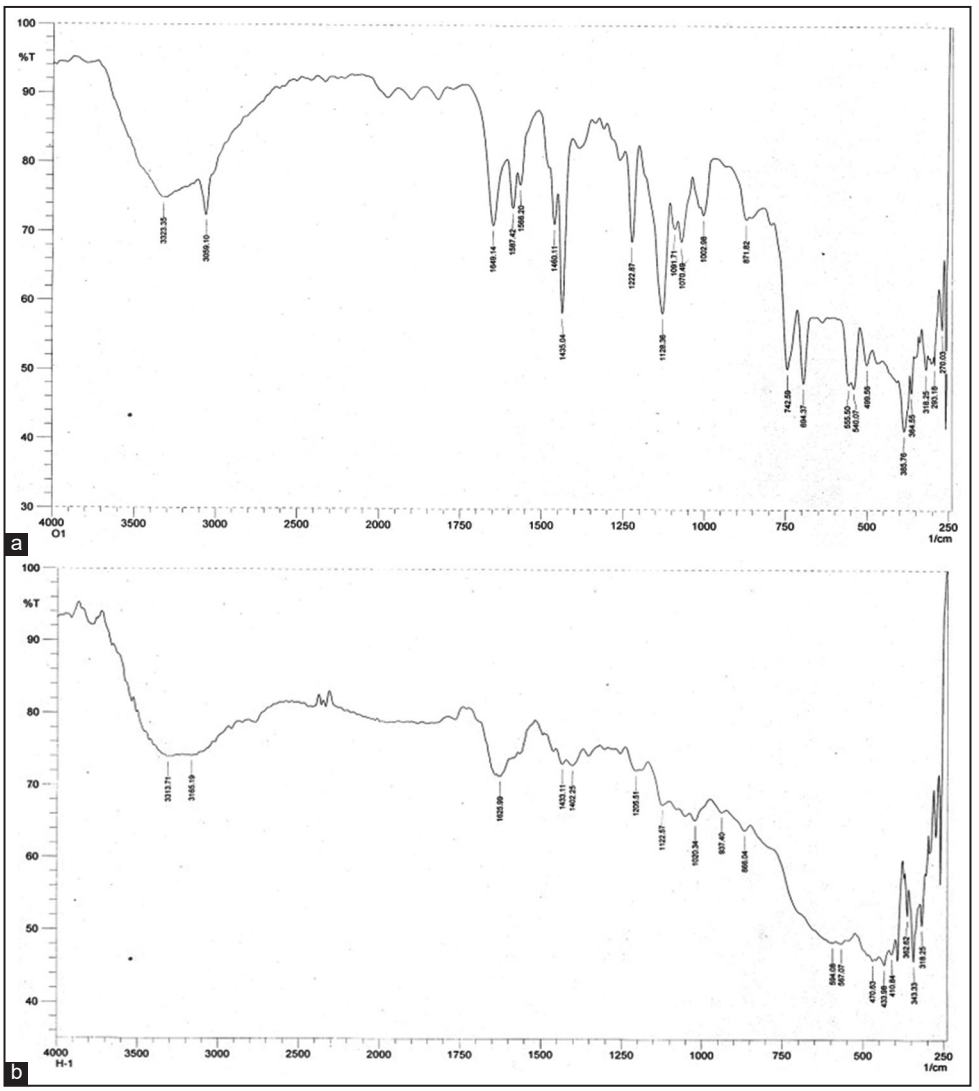

Figure 1: Fourier transform infrared spectra of (a) $[FeCl_2(\eta^2\text{-P,N-PPh}_2Py)_2]$ (**1**) and (b) $[FeCl_2(\eta^2\text{-P,P-DPEphos})_2]$ (**2**) complex.

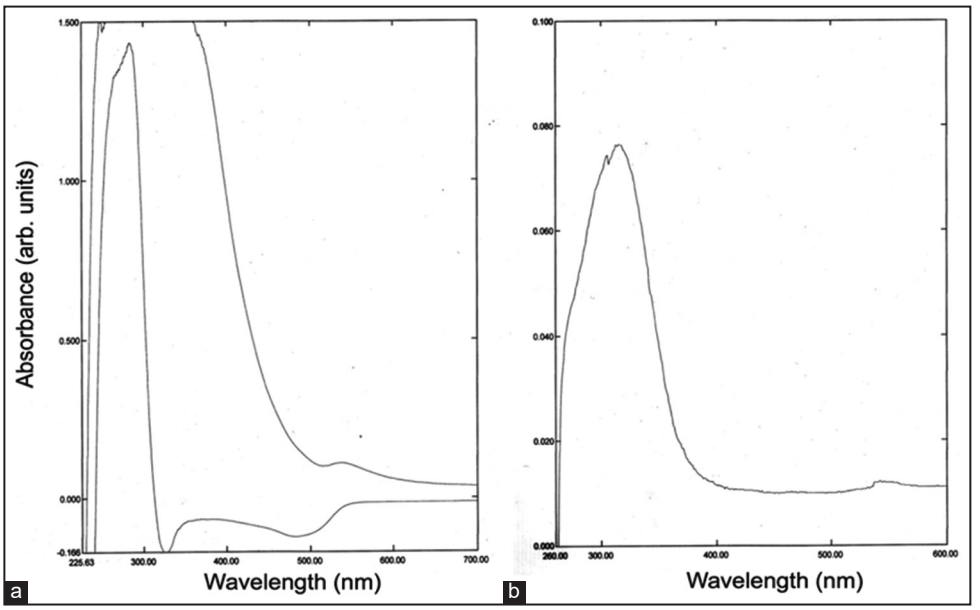

Figure 2: Ultraviolet-Vis spectrum of (a) $[FeCl_2(\eta^2\text{-P,N-PPh}_2Py)_2]$ (**1**) and (b) $[FeCl_2(\eta^2\text{-P,P-DPEphos})_2]$ (**2**) complexes.

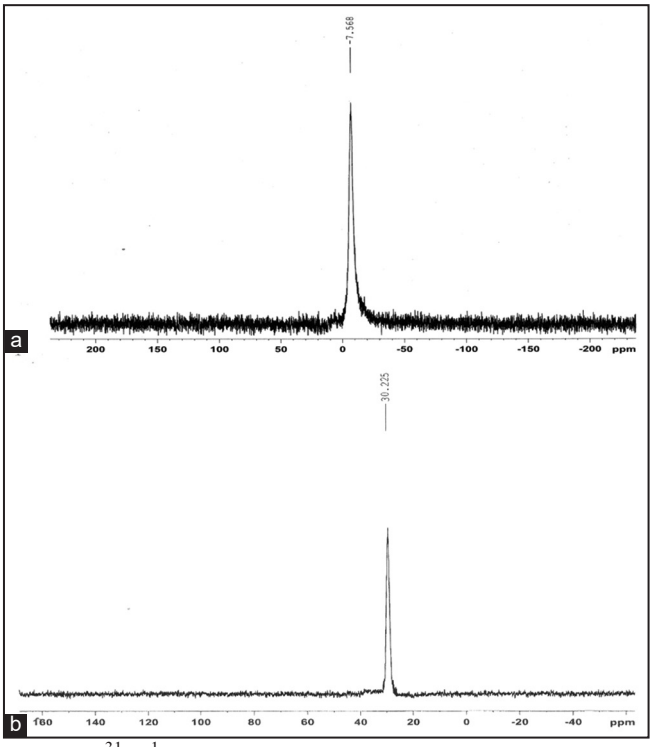

Figure 3: $^{31}P\{^1H\}$ Nuclear magnetic resonance spectra of (a) $[FeCl_2(\eta^2\text{-P,N-PPh}_2Py)_2]$ (**1**) and (b) $[FeCl_2(\eta^2\text{-P,P-DPEphos})_2]$ (**2**) complexes.

The $^{31}P\{^1H\}$ NMR spectrum of $[FeCl_2(\eta^2\text{-P,P-DPEphos})_2]$ (**2**) shows a singlet at about δ 30 ppm, shifting downfield compared to free ligand (δ–16.5 ppm) [47] confirming the coordination of P–atoms with the metal [Figure 3b]. The ^1H NMR spectrum shows a slightly broad peak for aromatic protons in the region δ 5.29–5.13 ppm [Supporting Information, Figure S6].

3.5. Structural Properties of the Complexes

In our theoretical calculations, we optimized the geometries of the two complexes in both *cis*- and *trans*-configurations. The *cis*-isomer of complex **1** and *trans*-isomer of complex **2** are predicted to the minimum energy (stable) geometries as shown in Figure 4. Geometry optimization of complexes **1** and **2** in the gas phase at the three spin states (S = 1/2, 3/2, and 5/2) confirms the high-spin quintet (S = 5/2) state to the minimum energy configuration. Structural parameters of the complexes such as bond length, bond angle, dipole moment, and HOMO-LUMO energy gap are provided in Table 1. We calculated that the relative stability of the complexes in terms of the total energy and quintet state is shown to be the ground state geometry for both complexes in their respective isomeric forms [Supporting Information, Table S2]. However, the energy difference between *cis*- and *trans*-isomers is found to be minimal. For complex **1**, although quintet spin state is shown to have favorable energy, it led to a significant elongation in Fe–P bond length to ~3.55 Å which is beyond the reported Fe–P bond length. Due to this reason, we considered a singlet (S = 1/2) spin state which shows reasonable agreement in the calculated geometric parameters. The total energies and relative stability of the isomers of complexes **1** and **2** in spin states 1/2, 3/2, and 5/2 are provided in Supporting Information, Table S2.

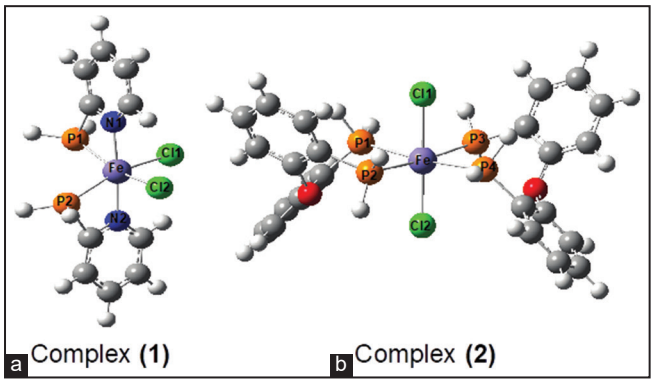

Figure 4: Minimum energy geometries of Fe(II) complexes **1** and **2** with hemilabile ligands. (a) Complex **1** in *cis*-configuration and (b) complex **2** in *trans*-configuration. Frequency calculations confirmed the ground state of the optimized structures in the gas phase.

In complexes **1** and **2**, the average Fe–P bond length is calculated to be ~2.39 Å and ~2.69 Å, respectively. The calculated bond lengths

Table 1: Geometrical parameters of the *cis*-isomer of complex 1 and *trans*-isomer of complex 2 calculated at the B3LYP/LANL2DZ/6-31+G(d,p) level of theory in the gas phase.

Complex	Bond length (Å)		Bond angle (°)		Dipole moment (D)	Energy gap (eV)
Complex 1	Fe–Cl1	2.38	Cl1-Fe-Cl2	128.92	8.97	3.79
	Fe–Cl2	2.38	Cl1-Fe-P1	80.20		
	Fe–P1	2.39	Cl2-Fe-P2	80.25		
	Fe–P2	2.39	N1-Fe-Cl1	102.80		
	Fe–N1	2.01	N2-Fe-Cl2	102.78		
	Fe–N2	2.01	P1-Fe-P2	75.47		
Complex 2	Fe–Cl1	2.42	Cl1-Fe-Cl2	180.0	0.07	4.80
	Fe–Cl2	2.37	Cl1-Fe-P1	92.66		
	Fe–P1	2.68	Cl2-Fe-P2	86.37		
	Fe–P2	2.70	Cl1-Fe-P3	93.63		
	Fe–P3	2.70	Cl2-Fe-P4	87.34		
	Fe–P4	2.68	P1-Fe-P2 P3-Fe-P4	89.45		

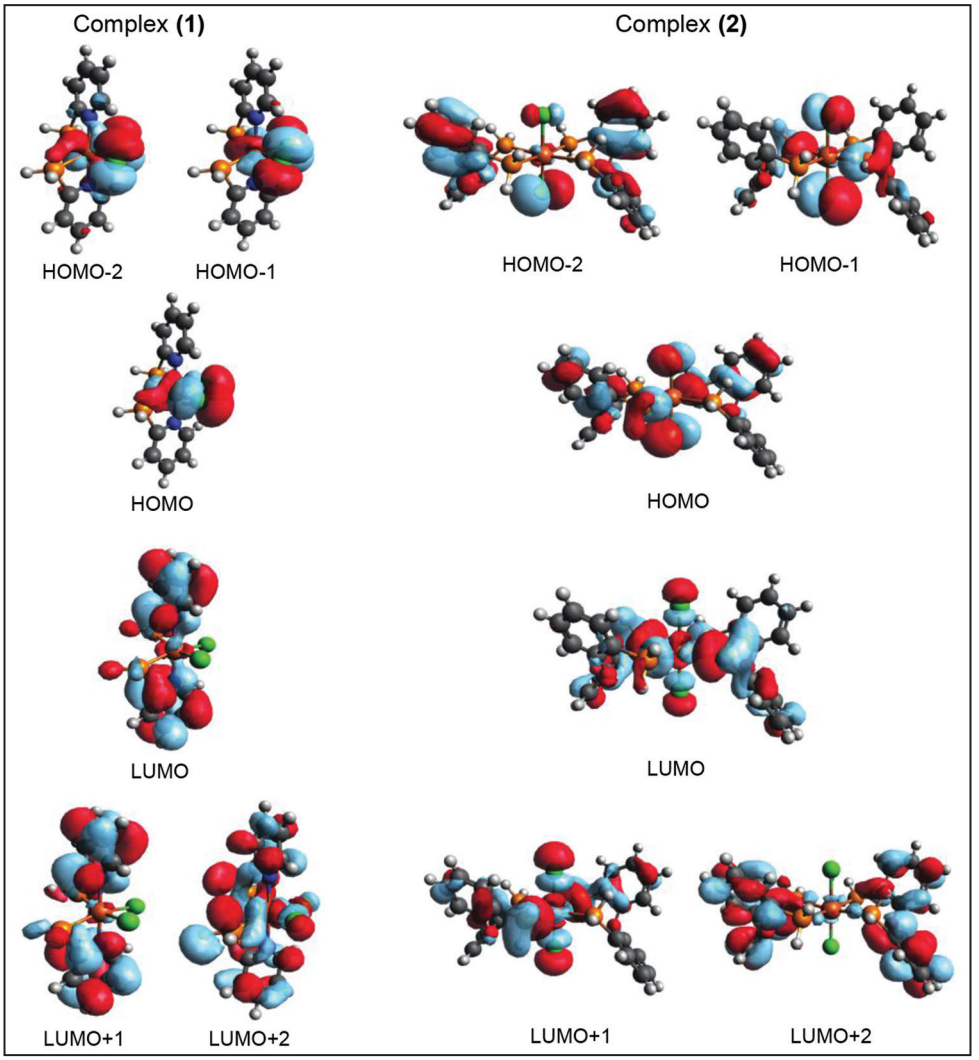

Figure 5: Frontier molecular orbitals corresponding to highest occupied molecular orbital (HOMO)-2, HOMO-1, HOMO, lowest unoccupied molecular orbital (LUMO), LUMO+1, and LUMO+2 of complexes **1** and **2** in the gas phase.

are longer when compared to the previously reported value of ~2.3 Å [35]. An elongation in Fe–P bond is observed in complex **2** which may be attributed to the quintet spin state of the complex. The Fe–P bond in complex **1**, *cis*-isomer, is shorter than in complex **2**, *trans*-

isomer. In a previous study by Kneebone *et al*. [48], Fe–P bond length in $FeCl_2$(bisphosphine) complexes was reported between 2.41 and 2.45 Å depending on the bisphosphine ligand coordinated to iron ion.

The average Fe–Cl bond length is calculated to be 2.38 Å for complex **1** and ~2.39 Å for complex **2**, which is in good agreement with previously reported value [35]. However, the calculated values are slightly longer than the reported $[FeCl_3\{PPh_2(p\text{-}C_6H_4NMe_2)\text{-}P\}_3]$ complex **1** and other known Fe-complex and these changes in the geometrical parameters may be attributed to electron delocalization [11,48,49]. The Fe–N bond length of 2.01Å in complex **1** is comparable to other known pyridyl complexes of Fe(III) [49]. Elongation in the calculated bond lengths, as shown in Table 1, is associated with the nature of the ligand coordinated to Fe(II) ion, the spin state of the complexes, electronic configuration, level of DFT calculation, and absence of intramolecular interactions, for example, van der Waals forces and hydrogen bond interactions in the gas phase DFT calculations [50,51].

3.6. Electronic Properties of the Complexes

The HOMO-LUMO energy gap is an important molecular descriptor in comparing the stability of transition metal complexes. A comparison of the HOMO-LUMO energy gap suggests complex **2** to have a higher energy gap of ~4.80 eV compared to complex **1** in the gas phase [Table 1], which can be attributed to the nature of ligand coordinated to Fe(II) ion. The smaller HOMO-LUMO energy gap in complex 1 clarifies the charge transfer interactions within the complex. In terms of dipole moment, we find that a deviation from a perfectly octahedral geometry leads to an increase in the overall dipole moment of the complex, as shown in Figure 4. The significantly higher dipole moment in complex **1** compared to complex **2** points to the former being more polarizable than complex **2**.

Frontier molecular orbitals suggest that in complex **1**, HOMO is mainly localized on atoms of chlorine and Fe while LUMO is delocalized on the ligand except for chlorine atoms [Figure 5]. In complex **2,** both HOMO and LUMO orbitals are localized on atoms of chlorine and Fe along with some contributions from the ligand. The frontier molecular orbitals for HOMO-1, HOMO-2, LUMO+1, and LUMO+2 are shown in Figure 5. In complex **1**, like HOMO orbitals, HOMO-1, and HOMO-2 are localized on the chlorine and Fe atoms. Thus, they act as electron donor sites in the complex. In complex **2**, both HOMO-1 and HOMO-2 are predominantly localized on chlorine atoms and delocalized on the aromatic ring which suggests these sites to contribute as electron donors in the complex. The LUMO+1 and LUMO+2 orbitals in complexes **1** and **2** are predominantly delocalized on the ligand with some contributions on Fe and chlorine atoms.

4. CONCLUSION

Two Fe(II) complexes with PPh_2Py and DPEphos ligands were synthesized and characterized using elemental analysis, ESI-mass, FTIR, UV-Vis, ^1H, and $^{31}P\{^1H\}$ NMR spectroscopy. Molecular geometries of the synthesized complexes were optimized in the gas phase using DFT calculations to get better insights into their structural and electronic properties. DFT calculations support the experimental findings by establishing the *cis*- and *trans*-isomers of complexes **1** and **2**, to be the most stable form of the complexes. Further, the spin state of the Fe(II) center is crucial in determining the stable geometry, isomeric forms, and interaction through the ancillary ligand. As literature reports on synthesized complexes with Fe(II) are rather limited, the present study extends the scope of Fe(II) complexes with a large bite angle diphosphine ligand and a small bite angle PPh_2Py ligand and highlights the importance and potential relevance of phosphine-based ligands in iron chemistry.

5. DECLARATION OF COMPETING INTEREST

The authors declare that they have no known competing financial interests or personal relationships that could have appeared to influence the work reported in this paper.

6. ACKNOWLEDGMENT

The services of SAIF (NEHU), Shillong, are gratefully acknowledged for the NMR and ESI-mass analysis.

7. SUPPORTING INFORMATION

The elemental analytical data of Fe(II) complexes, the experimentally measured ESI-Mass and ^1H NMR spectrum of $[FeCl_2(\eta^2\text{-}P,N\text{-}PPh_2Py)_2]$ **(1)** and $[FeCl_2(\eta^2\text{-}P,P\text{-}DPEphos)_2]$ **(2)** complexes. DFT calculated total electronic energies and relative energies of complexes **(1)** and **(2)** in three different spin states: 1/2, 3/2, and 5/2, respectively.

8. REFERENCES

1. S. M. Kuang, Z. Z. Zhang, B. M. Wu, T. C. W. Mak, (1997) Synthesis of Fe-M complexes (M = Mo, Mn, Fe, Co, Ni, Zn, Cd, Hg) using *trans*-$Fe(EtPhPpy)_2(CO)_3$ as an organometallic tridentate ligand molecular structures of $(CO)_3Fe(\mu\text{-}EtPhPpy)_2Mo(CO)_3$ and $(CO)_3Fe(\mu\text{-}EtPhPpy)_2Cd(SCN)_2$ (EtPhPpy = 2-(ethylphenylphosphino)pyridine), ***Journal of Organometallic Chemistry***, **540:** 55-60.
2. G. R. Newkome, (1993) Pyridylphosphines, ***Chemical Reviews***, **93:** 2067-2089.
3. P. Braunstein, M. Knorr, M. Strampfer, A. DeCian, J. Fischer, (1994) Synthetic, spectroscopic and structural studies on phosphine-stabilised [PPh_3, $Ph_2PCH_2PPh_2$, $Ph_2P(CH_2)_4PPh_2$, $(Ph_2P)C_5H_4N$] main group element-iron-silicon chain complexes, ***Journal of the Chemical Society, Dalton Transactions***, **2**: 117-134.
4. H. G. Ang, W. L. Kwik, P. T. Lau, (1990) Coordinating properties of 2-pyridyldiphenylphosphine with some metal carbonyls, ***Polyhedron***, **9:** 1479-1482.
5. K. Nishide, S. Ito, M. Yoshifuji, (2003) Preparation of carbonyltungsten(0) complexes of 2-pyridylphosphines showing a stepwise coordination pattern by way of monodentate to chelate mode, ***Journal of Organometallic Chemistry***, **682:** 79-84.
6. K. Wajda-Hermanowicz, Z. Ciunik, A. Kochel, (2006) Syntheses and molecular structure of some Rh and Ru complexes with the chelating Diphenyl (2-Pyridyl)p hosphine Ligand, ***Inorganic Chemistry***, **45:** 3369-3377.
7. A. J. Deeming, M. B. Smith, (1993) Triosmium clusters with 2-pyridylphosphines as ligands, ***Journal of the Chemical Society, Dalton Transactions***, **22:** 3383-3391.
8. G. Francio, R. Scopelliti, C. G. Arena, G. Bruno, D. Drommi, F. Faraone, (1998) IrPd, IrHg, IrCu, and IrTl Binuclear Complexes Bridged by the Short-Bite Ligand 2-(Diphenylphosphino)pyridine. Catalytic Effect in the Hydroformylation of Styrene Due to the Monodentate P-Bonded 2-(Diphenylphosphino)pyridine Ligands of trans-$[Ir(CO)(Ph_2PPy)_2Cl]$, ***Organometallics***, **17:** 338-347.
9. S. M. Kuang, F. Xue, Z. Z. Zhang, W. M. Xue, C. M. Che, T. C. W. Mak, (1997) A novel luminescent iridium(I)-cadmium(II) binuclear complex displaying a long-lived metal-to-ligand charge-transfer excited state. Synthesis and structural characterization of $I(CO)_2Ir(\mu\text{-}Ph_2Ppy)_2CdI_2$ [Ph_2Ppy = 2-(diphenylphosphino) pyridine], ***Journal of the Chemical Society, Dalton Transactions***, **19**: 3409-3410.
10. E. C. Carson, S. J. Lippard, (2006) Dioxygen-Initiated oxidation

of heteroatomic substrates incorporated into ancillary pyridine ligands of carboxylate-rich Diiron(II) complexes, ***Inorganic Chemistry***, **45:** 837-848.
11. P. Das, P. P. Sarmah, M. Borah, A. K. Phukan, (2009) Low-spin, mononuclear, Fe(III) complexes with P,N donor hemilabile ligands: A combined experimental and theoretical study, ***Inorganica Chimica Acta***, **362:** 5001-5011.
12. Y. Takahashi, N. Murakami, K. I. Fujita, R. Yamaguchi, (2009) Synthesis and reactivity of homo- and hetero-dimetallic complexes bridged by diphenyl-2-pyridylphosphine and hydrides: Regioselectivity of alkyne insertion into unsaturated M^1(micro-PPh_2Py)(micro-$H)_2M^2$ moieties, ***Dalton Transactions***, **11**: 2029-2042.
13. A. J. Deeming, M. B. Smith, (1993) Cleavage of phosphorus-phenyl and phosphorus-2-pyridyl bonds in the reactions of mixed phenyl-(2-pyridyl) phosphines with [$Ru_3(CO)_{12}$], ***Journal of the Chemical Society, Dalton Transactions***, **13**: 2041-2046.
14. M. N. Birkholz, Z. Freixa, P. W. N. M. Van Leeuwen, (2009) Bite angle effects of diphosphines in C-C and C-X bond forming cross coupling reactions, ***Chemical Society Reviews***, **38:** 1099-1118.
15. R. Venkateswaran, M. S. Balakrisna, S. M. Mobin, H. M. Tuononen, (2007) Copper(I) complexes of Bis(2-(diphenylphosphino) phenyl) ether: Synthesis, reactivity, and theoretical calculations, ***Inorganic Chemistry***, **46:** 6535-6541.
16. M. A. Zuideveld, B. H. G. Swennenhuis, M. D. K. Boele, Y. Guari, G. P. F. Van Strijdonck, J. N. H. Reek, P. C. J. Kamer, K. Goubitz, J. Fraanje, M. Litz, A. L. Spek, P. W. N. M. Van Leeuwen, (2002) The coordination behavior of large natural bite angle diphosphine ligands towards methyl and 4-cyanophenylpalladium(II) complexes, ***Journal of the Chemical Society, Dalton Transactions***, **11**: 2308-2317.
17. R. Venkateswaran, J. T. Mague, M. S. Balakrisna, (2007) Ruthenium(II) Complexes Containing Bis(2-(diphenylphosphino) phenyl) Ether and their catalytic activity in hydrogenation reactions, ***Inorganic Chemistry***, **46:** 809-817.
18. S. M. Kuang, P. E. Fanwick, R. A. Walton, (2002) Unsymmetrical Dirhenium complexes that contain [Re(2)](6+) and [Re(2)](5+) cores complexed by tridentate ligands with P(2)O and P(2)N donor sets, ***Inorganic Chemistry***, **41:** 405-412.
19. D. Freudenmann, C. Feldmann, (2011) Ionic liquid based Synthesis of the dinuclear complex Ag_2I_2(DPEphos)$_2$ with Ag-Ag interaction, ***Inorganica Chimica Acta***, **375:** 311-313.
20. P. Aslanidis, P. J. Cox, A. C. Tsipis, (2010) Structural and electronic properties of luminescent copper(I) halide complexes of bis[2-(diphenylphosphano)phenyl]ether (DPEphos). Crystal structure of [CuCl(DPEphos)(dmpymtH], ***Dalton Transactions***, **39:** 10238-10248.
21. L. Zhang, B. Li, (2009) A series of 4,5-diazafluoren-9-one-derived ligands and their Cu(I) complexes: Synthesis, characterization and photophysical properties, ***Inorganica Chimica Acta***, **362:** 4857-4861.
22. S. M. Kuang, D. G. Cuttell, D. R. McMillin, P. E. Fanwick, R.A. Walton, (2002) Synthesis and structural characterization of Cu(I) and Ni(II) complexes that contain the bis[2-(diphenylphosphino) phenyl]ether ligand. Novel emission properties for the Cu(I) species, ***Inorganic Chemistry***, **41:** 3313-3322.
23. J. Wilting, C. Muller, A. C. Hewat, D. D. Ellis, D. M. Tooke, A. L. Spek, D. Vogt, (2005) Nickel-catalyzed isomerization of 2-methyl-3-butenenitrile, ***Organometallics*** **24:** 13-15.
24. Z. H. Guan, Z. H. Ren, S. M. Spinella, S. Yu, Y. M. Liang, X. Zhang, (2009) Rhodium-catalyzed direct oxidative carbonylation of aromatic C-H BOND with CO and alcohols, ***Journal of the American Chemical Society***, **131(2)**: 729-733.
25. X. F. Wu, H. (2012) Neumann, ruthenium and rhodium-catalyzed carbonylation reactions, ***ChemCatChem***, **4:** 447-458.
26. M. S. Balakrisna, R. Venkateswaran, S. M. Mobin, (2008) Silver(I) complexes of bis[2-(diphenylphosphino)phenyl] ether, ***Polyhedron***, **27:** 899-904.
27. M. Kranenburg, J. G. P. Delis, P. C. J. Kamer, P. W. N. M. Van Leeuwen, K. Vrieze, N. Veldman, A. L. Spek, K. Goubitz, J. Fraanje, (1997) Palladium(0)-tetracyanoethylene complexes of diphosphines and a dipyridine with large bite angles and their crystal structures., ***Dalton Transactions***, **11**: 1839-1850.
28. B. Dudle, K. Rajesh, O. Blacque, H. Berke, (2011) Rhenium in homogeneous catalysis: [ReBrH(NO)(labile ligand)(large-bite-angle diphosphine)] complexes as highly active catalysts in olefin hydrogenations, ***Journal of the American Chemical Society***, **133:** 8168-8178.
29. B. Dudle, K. Rajesh, O. Blacque, H. Berke, (2011) Rhenium nitrosyl complexes bearing large-bite-angle diphosphines, ***Organometallics***, **30:** 2986-2992.
30. M. L. Parr, C. Perez-Acosta, J. W. Faller, (2005) Synthesis, characterization and structural investigation of new rhenium-oxo complexes containing bidentate phosphine ligands: An exploration of chirality and conformation in chelate rings of small and large bite angle ligands, ***New Journal of Chemistry***, **29:** 613-619.
31. S. Hanf, L. A. Rupflin, R. Glaser, S. A. Schunk, (2020) Current state of the art of the solid rh-based catalyzed hydroformylation of short-chain olefins, ***Catalysts***, **10(5)**: 510.
32. B. C. Hamann, J. F. Hartwig, (1998) Systematic variation of bidentate ligands used in aryl halide amination. Unexpected effects of steric, electronic and geometric perturbations, ***Journal of the American Chemical Society***, **120:** 3694-3703.
33. J. P. Sadighi, M. C. Harris, S. L. Buchwald, (1998) A highly active palladium catalyst system for the arylation of anilines, ***Tetrahedron Letters***, **39:** 5327-5330.
34. E. G. Dennis, D. W. Jeffery, M. V. Perkins, P. A. Smith, (2011) Pd(DPEPhos)Cl_2-catalyzed Negishi cross-couplings for the formation of biaryl and diarylmethane phloroglucinol adducts, ***Tetrahedron***, **67:** 2125-2131.
35. M. Borah, N. Saikia, P. Das, (2021) A combined computational and experimental study of Fe(II) complexes with hemilabile phosphine-based P,O donor ligands, ***Journal of Molecular Structure***, **1230:** 129661.
36. M. J. Frisch, G. W. Trucks, H. B. Schlegel, G. E. Scuseria, M. A. Robb, J. R. Cheeseman, G. Scalmani, V. Barone, B. Mennucci, G. A. Petersson, H. Nakatsuji, M.Caricato, X. Li, H. P. Hratchian, A. F. Izmaylov, J. Bloino, G. Zheng, J. L. Sonnenberg, M. Hada, M. Ehara, K. Toyota, R. Fukuda, J. Hasegawa, M. Ishida, T. Nakajima, Y. Honda, O. Kitao, H. Nakai, T. Vreven, J. A. Jr. Montgomery, J. E. Peralta, F. Ogliaro, M. Bearpark, J. J. Heyd, E. Brothers, K. N. Kudin, V. N. Staroverov, T. Keith, R. Kobayashi, J. Normand, K. Raghavachari, A. Rendell, J. C. Burant, S. S. Iyengar, J. Tomasi, M. Cossi, N. Rega, J. M. Millam, M. Klene, J. E. Knox, J. B. Cross, V. Bakken, C. Adamo, J. Jaramillo, R. Gomperts, R. E. Stratmann, O. Yazyev, A. J. Austin, R. Cammi, C. Pomelli, J. W. Ochterski, R. L. Martin, K. Morokuma, V. G. Zakrzewski, G. A. Voth, P. Salvador, J. J. Dannenberg, S. Dapprich, A. D. Daniels, Ö.Farkas, J. B. Foresman, J. V. Ortiz, J. Cioslowski, D. J. Fox, (2010) ***Gaussian 09***, Wallingford, CT: Gaussian, Inc.
37. P. J. Hay, W. R. Wadt, (1985) Ab initio effective core potentials

for molecular calculations. Potentials for K to Au including the outermost core orbitals, ***The Journal of Chemical Physics***, **82:** 299-310.
38. D. H. Wells, W. N. Delgass, K. T. Thomson, (2002) Density functional theory investigation of gold cluster geometry and gas-phase reactivity with O_2, ***The Journal of Chemical Physics***, **117:** 10597.
39. M. H. Abdalmoneam, K. Waters, N. Saikia, R. Pandey, (2017) Amino-acid-conjugated gold clusters: Interaction of alanine and tryptophan with Au_8 and Au_{20}, ***The Journal of Physical Chemistry***, **121:** 25585-25593.
40. H. Grönbeck, W. Andreoni, (2000) Gold and platinum microclusters and their anions: Comparison of structural and electronic properties, ***Chemical Physics***, **262:** 1-14.
41. M. G. Amiri, H. Golchoubian, (2018) Solvatochromism, thermochromism and density functional theory studies of Copper(II) complexes containing hemilabile tetradentate ligand, ***Journal of Molecular Structure***, **1165:** 196-205.
42. M. D. Hanwell, D. E. Curtis, D. C. Lonie, T. Vandermeersch, E. Zurek, G. R. Hutchison, (2012) Avogadro: An advanced semantic chemical editor, visualization, and analysis platform, ***Journal of Cheminformatics***, **4**:17.
43. P. T. Ndifon, M. O. Agwara, Y. Hayashi, A. Uehara, (2008) Synthesis and characterisation of some metal complexes of hybrid phosphorus-nitrogenligands: The crystal structure of 1-(diphenylphosphino)-2-(2-pyridyl)ethane cobalt(II) chloride, ***Bulletin of the Chemical Society of Ethiopia***, **22:** 253-260.
44. K. Nakamoto, (1970) ***Infrared Spectra of Inorganic and Coordination Compounds***, 2nd ed. United States: John Wiley and Sons.
45. S. O. Grim, J. D. Mitchell, (1977) Unsymmetrical bis-phosphorus ligands. 9. Group VI metal carbonyl complexes and other derivatives of various (phosphinomethyl)phosphine sulfides, ***Inorganic Chemistry***, **16:** 1762-1770.
46. R. Rojas, M. Valderrama, (2004) Trimethylsilylcyclopentadienylchromium(III) complexes with diphenyl-2-pyridylphosphine: Synthesis, structural characterisation and catalytic behaviour of $[(C_6H_5)_2PC_5H_4NH][(\eta^5\text{-}Me_3SiCp)CrCl_3]$, ***Journal of Organometallic Chemistry***, **689:** 2268-2272.
47. W. K. Wong, L. Zhang, W. T. Wong, (1998) Synthesis and X-ray crystal structure of a hexanuclear silver(I) complex with non-chelating tri- and tetradentate bridging o-(diphenylphosphino) benzoate ligands, ***Chemical Communications***, **6**: 673-674.
48. J. L. Kneebone, V. E. Fleischauer, S. L. Daifuku, A. A. Shaps, J. M. Bailey, T. E. Iannuzzi, M. L. Neidig, (2016) Electronic structure and bonding in Iron(II) and Iron(I) complexes bearing bisphosphine ligands of relevance to iron-catalyzed C-C Cross-coupling, ***Inorganic Chemistry***, **55:** 272-282.
49. D. Mandon, A. Nopper, T. Litrol, S. Goetz, (2001) Tridentate coordination of monosubstituted derivatives of the tris(2-pyridylmethyl)amine ligand to $FeCl_3$: Structures and spectroscopic properties of ((2-Bromopyridyl)methyl)bis-(2-pyridylmethyl) amine Fe(III)Cl_3 and (((2-p-Methoxyphenyl)pyridyl)methyl) Bis(2-pyridyl-methyl)]amine Fe(III)Cl_3 and Comparison with the Bis(2-pyridylmethyl)]amine Fe(III)Cl_3 Complex, ***Inorganic Chemistry***, **40:** 4803-4806.
50. Z. Shaghaghi, R. Bikas, H. Tajdar, A. (2020) Kozakiewicz, Iron(III) complexes with N_2O_2-donor salophen and azide ligands: Crystal structure, experimental and theoretical studies, ***Journal of Molecular Structure***, **1217:** 128431-128439.
51. A. Masoudiasl, M. Montazerozohori, S. Joohari, L. Taghizadeh, G. Mahmoudi, A. Assoud, (2019) Structural investigation of a new cadmium coordination compound prepared by sonochemical process: Crystal structure, Hirshfeld surface, thermal, TD-DFT and NBO analyses, ***Journal of Molecular Structure***, **52:** 244-256.

****Bibliographical Sketch***

Dr. Nabanita Saikia is an Assistant Professor of Physical/Computational Chemistry at New Mexico Highlands University. Dr. Saikia holds a Ph.D. in Computational and Theoretical Chemistry from Tezpur University, India, and has extensive experience in computational chemistry and molecular modeling. Dr. Saikia's primary research interests lie in understanding the conformational dynamics and structural ensembles of intrinsically disordered proteins and signaling scaffold proteins. She is also interested in studying the molecular recognition and self-assembly of biomolecules on nanomaterial interfaces, and molecular modeling of functional nanomaterials for drug delivery applications. Dr. Saikia has authored several peer-reviewed publications in scientific journals and currently serves as an Associate Editor for Molecular Recognition, Frontiers in Molecular Biosciences journal. Additionally, she serves as a Review Editor for a) Coacervates and Biological Condensates, Frontiers in Biophysics, and b) Structural Biology, Frontiers in Molecular Biosciences journals. Dr. Saikia was elected a full member of Sigma Xi, The Scientific Research Honor Society in 2023